

Saclay T01/126
hep-ph/0111335

Supernovae as a Probe of Particle Physics and Cosmology

JOSHUA ERLICH^a and CHRISTOPHE GROJEAN^b

^a *Theory Division T-8, Los Alamos National Laboratory, Los Alamos, NM 87545, USA*

^b *Service de Physique Théorique, CEA-Saclay, F-91191 Gif-sur-Yvette, France*

`erlich@lanl.gov, grojean@spht.saclay.cea.fr`

Abstract

It has very recently been demonstrated by Csáki, Kaloper and Terning (CKT) that the faintness of supernovae at high redshift can be accommodated by mixing of a light axion with the photon in the presence of an intergalactic magnetic field, as opposed to the usual explanation of an accelerating universe by a dark energy component. In this paper we analyze further aspects of the CKT mechanism and its generalizations. The CKT mechanism also passes various cosmological constraints from the fluctuations of the CMB and the formation of structure at large scales, without requiring an accelerating phase in the expansion of the Universe. We investigate the statistical significance of current supernova data for pinning down the different components of the cosmological energy-momentum tensor and for probing physics beyond the standard model.

1 Introduction

The dynamics of the Universe in the standard cosmological model is completely determined by the present values ⁽¹⁾ of the Hubble parameter, H_0 , and the ratios Ω_{0i} between the energy density of the different “matter” components and the critical density. The task assigned to cosmologists by Sandage is the precise determination of these numbers. Unfortunately, they are not directly measurable and their determination relies on the measurement of quantities indirectly dependent on them. Several bounds on the Ω_{0i} follow from the study of the anisotropies of the cosmic microwave background radiation (CMB), the formation of large scale structure, the age of the Universe, *etc.* The Hubble diagrams (luminosity distances vs. redshifts) of standard candles have traditionally been a useful tool for determining constraints on some of the cosmological parameters. Perhaps the most astonishing physical result of the past few years [1, 2] is that not only is the Hubble diagram of high redshift supernovae (SNe) compatible with previous independent constraints on the Ω_{0i} , but it is also complementary to them and in principle allows a complete determination ($H_0 \sim 66 \text{ km.s}^{-1}.\text{Mpc}^{-1}$, $\Omega_{0m} \sim .3$ and $\Omega_{0\Lambda} \sim .7$). In particular this result reveals the presence of a so-called “dark energy” component accounting for the dimming of high- z SNe as a result of a current period of acceleration in the expansion of the Universe. However, both the existence as well as the size of this Dark Energy component jeopardize our current understanding of the fundamental laws of particle physics [3] and string theory/quantum gravity [4].

Very recently Csáki, Kaloper and Terning (CKT) [5] have proposed an interesting alternative explanation of combined Type Ia supernova data from the Calán-Tololo [6] survey, the Supernova Cosmology Project (SCP) [2], and the High- z Supernova Search Team (HZT) [1] without requiring a period of accelerating expansion. By assuming the existence of a light axion ϕ ($m_\phi \sim 10^{-16} \text{ eV}/c^2$) and an intergalactic magnetic field of amplitude $|\mathbf{B}| \sim 10^{-13}$ Tesla, the authors of [5] found that the magnitude-redshift curve corresponding to the best fit flat universe with a cosmological constant [2] ($\Omega_{0m} \sim 0.28$, $\Omega_{0\Lambda} \sim 0.72$) can be closely reproduced with cosmic strings replacing the cosmological constant. The axion interacts with photons via a term in the effective Lagrangian of the form, $\mathcal{L}_{int} = \frac{1}{M_L c^2} \phi \mathbf{E} \cdot \mathbf{B}$, where ϕ is the axion field and M_L is the axion coupling mass scale, which CKT fit to $M_L \sim 4 \cdot 10^{11} \text{ GeV}/c^2$. As a result of this coupling, photons and axions will oscillate in a background magnetic field via a Primakoff effect. Assuming a randomly oriented magnetic field with a coherence length of the order of 1 Mpc, almost one third of the highest redshift photons would decay by the time they reach us.

In this letter we study the statistical significance of the CKT results, and discuss possible generalizations of the CKT mechanism. In order to understand the model dependence of generalized photon loss mechanisms we use the supernova data to identify the allowed regions in the parameter space of such models, obtaining fits at least as good as those of the cosmological constant accelerating universe. The anisotropy of the CMB

⁽¹⁾A subscript 0 will always denote the value taken today by any quantity.

still requires a Dark Energy component to the energy-momentum tensor. The large scale structure of the Universe then imposes constraints on the equation of state of the invisible Dark Energy. The difference from previous analyses is that the SN data now allows for a significantly larger range of the equation of state parameter w_X (in $p = w_X \rho$) for the Dark Energy component. It is interesting that the preferred region for w_X remains in the range $w_X < 0$, in agreement with requirements of large scale structure. The key point is that instead of indicating an accelerating expansion of the Universe, the dimming of SNe at high redshift would reveal the presence of a light axion which mixes with photons in the intergalactic medium.

Because this subject unites several branches of theory and experiment which some readers may not be familiar with, in Section 2 we briefly review the relevant experiments and current bounds on the relevant cosmological and particle physics parameters. In Section 3 we review the theoretical basis of the CKT photon loss mechanism and its generalizations. This mechanism is intrinsically quantum mechanical, as opposed to the essentially classical models of photon absorption by dust [7]. We then describe in Section 4 the constraints placed on the cosmological parameters by the Hubble diagrams of type Ia SNe and how they are modified in the presence of a photon loss mechanism.

In Section 5 we perform a statistical analysis of the data and our fits, and demonstrate that the CKT model with a best fit photon decay parameter (with $\Omega_{0m} = .3$, $\Omega_{0X} = .7$, $w_X = -1/3$) is as good as the $\Omega_{0m} = .28$, $\Omega_{0\Lambda} = .72$ cosmological constant accelerating universe scenario. We present some exclusion regions of the parameter space, but there is a large range of allowed parameters for a generalized CKT mechanism to accommodate the data.

We conclude with proposals for future experiments to better pin down the Sandage numbers and ferret out the nature of the Dark Energy, and perhaps reveal the existence of an axion coupled to the particles of the Standard Model or other new physics beyond the standard model.

2 Experiments and bounds

In this section we summarize experimental bounds on and estimates of the relevant cosmological, astrophysical and particle physics parameters.

2.1 Cosmological Constraints

Although the energy density ratios Ω_{0i} are not directly measurable, they affect the time evolution of the scale factor of the Universe which in turn controls at least three types of measurable quantities: (i) the growth of density perturbations responsible for the formation of structure at large scales; (ii) the age of the Universe; (iii) the propagation of light between its emission by some known astrophysical sources and its detection today.

The sequence of structure formation starting from smaller fluctuations and ending with clusters of galaxies is well described by cold dark matter models, and the structure observed today could well have evolved from the density perturbations revealed by the CMB anisotropy at $z \sim 1000$. The presence of Dark Energy should not inhibit the growth of density perturbations, which implies that the Dark Energy should have started to dominate only recently. This requires an upper bound on ω_X at least as strong as $\omega_X < \omega_m = 0$ [8, 9].

The fluctuations in the CMB can also be used to predict the distribution of matter, baryon and Dark Energy in the Universe. The position of the first peak in the power spectrum as a function of multipole moment depends on the total density ($\Omega_{0m} + \Omega_{0X}$) and also less sensitively on Ω_{0m} and $\Omega_{0\text{baryon}}$. The latest determination by the BOOMERANG experiment is about $\Omega_0 = 1.0 \pm 0.1$ and $\Omega_{0m} \sim .33 \pm .03$ (and only a small fraction of baryons) [10]. The flat universe is heavily favored by this observation, as any deviation from flatness tends to grow quickly in Big Bang cosmology. This observational result as well as a nearly scale-invariant spectrum of primeval density perturbations is in accordance with the predictions of inflationary models. The estimate of Ω_{0m} seems also in agreement, at least for its order of magnitude, with the measures of mass-to-light ratios in clusters. Even if the CMB cannot directly teach us about the Dark Energy (the CMB is an image of the Universe at $z \sim 1000$ where the Dark Energy was completely washed out), it still points out a missing component of the energy-momentum tensor.

Some other cosmological constraints, for example from the age of the Universe or gravitational lensing, are less predictive due to high uncertainties and limited data.

Finally, we can determine some cosmological constraints from the Hubble diagrams of some “standard candle” sources: if we know the absolute luminosity of the source, by measuring the flux we receive today, we can deduce the distance travelled by the light, and this distance depends on the Ω_{0i} ratios. At very low redshift ($z < .1$), this dependence is however universal while at large redshift ($z \sim 5$) all the components with $\omega_i < 0$ have been washed out by the matter energy density. The intermediate interval is thus the best suited to bring some information on the Dark Energy. Among the astrophysical objects observed in this redshift interval are the type Ia supernovae. And by chance, Type Ia supernovae have been found to be decent standard candles by means of matching luminosity vs. time curves to the phenomenological Phillips curve [11]. As we will explain in detail later, the information on the cosmological parameters inferred from the Hubble diagrams relies on the nature of the propagation of light. Assuming a free propagation of the photons in the cosmological background, and assuming a flat universe, the best fit of the SN data gives [2] $\Omega_{0m} = 0.28 \pm 0.09$. This is in good agreement with several other determinations, which is perhaps why the relatively poor current statistics in high- z supernova data is sometimes overlooked. The aim of this work is to study how this conclusion is modified when the photons are no longer freely propagating but rather interact with an axion in such a way that some photons are lost between their emission by the SNe and their detection today. The following section will review the CKT photon loss mechanism and we will analyze the SN data taking into account such a photon loss mechanism in Section 5.

2.2 Astro-particle Constraints

The axion is a proposed ultralight pseudoscalar scalar field that would couple weakly with ordinary stable matter. The relevant coupling for the present study is that between axions and photons. The coupling is through a term in the Lagrangian of the form, $\mathcal{L} \supset \frac{1}{M_L c^2} \phi \mathbf{E} \cdot \mathbf{B}$, where ϕ is the axion and M_L is the axion coupling mass scale. Several searches for axions have turned up negative, placing constraints on the axion mass and couplings. In particular, a study of conversion of solar axions to X-rays in a strong magnetic field give $M_L > 1.7 \times 10^9 \text{ GeV}/c^2$ [13]. Based on mixing between axions and photons in an external magnetic field, precisely the effect needed for the CKT mechanism, studies of globular-cluster stars provide a rough limit $M_L > 1.7 \times 10^{10} \text{ GeV}/c^2$ [14]. For more complete reviews, see [15]. Bounds on the axion mass are closely tied to the axion coupling, but the absence of intergalactic line emissions and other experiments place a rough bound of $m_a < 10^{-3} \text{ eV}/c^2$ [16]. The CKT axion of mass $m_a \sim 10^{-16} \text{ eV}/c^2$ and coupling of $M_L \sim 4 \cdot 10^{11} \text{ GeV}/c^2$ is within current bounds.

The coupling between the axion and the photon requires the existence of the magnetic field. Magnetic fields appear to permeate the observable universe over a large range of scales, from relatively strong fields in the interstellar galactic medium, to weaker fields in the outer envelopes of X-ray clusters. The intergalactic magnetic field can be deduced by observations of radiation from relativistic electrons around X-ray clusters. These observations suggest an intergalactic magnetic field of around $B \sim 10^{-13} \text{ Tesla}$. (See [17, 18] for recent summaries.) The magnitude of the intergalactic magnetic field can also be estimated by other means, including studies of radio emission of distant quasars which, assuming a coherence length for the magnetic field of about 1 Mpc, yields roughly the same estimate [19]. The source of these magnetic fields is not well understood, but there have been several suggestions made, from inhomogeneous cosmological lepton number [20] to expanding quasar outflows [17]. Based on these results, CKT assumed a bulk magnetic field of 10^{-13} Tesla , and assumed a coherence length of 1 Mpc. The distribution and variation of the magnetic fields in the intergalactic medium is still not well understood. For a recent review of the relevant experiments and the significance of magnetic fields in the early universe, and for a more complete list of references, see [21].

3 CKT photon loss mechanism

Following the pioneering works [22] of Sikivie and Georgi, Ginsparg and Glashow, the CKT model considers an axion–photon coupling in the inter-galactic magnetic field ⁽²⁾

$$\mathcal{L}_{int} = \frac{1}{M_L c^2} \phi \mathbf{E} \cdot \mathbf{B} \quad (3.1)$$

where the scale M_L characterizes the strength of the axion–photon interactions. In a region where the magnetic field is approximately constant, the polarization of the photon whose electric field is parallel to the magnetic field mixes with the axion to form an oscillating system, much like that of the massive neutrino system. The mass eigenstates in the presence of the background magnetic field are not the same as the mass eigenstates in vacuum, and thus the photons oscillate into axions and *vice et versa*. A quantum mechanical computation gives the probability that a photon has not yet oscillated into an axion over a distance l as,

$$P_{\gamma \rightarrow \gamma}(l) = 1 - \frac{4 \mu^2 \epsilon^2}{m_\phi^4 c^8 + 4 \mu^2 \epsilon^2} \sin^2 \left((\sqrt{\epsilon^2 - \lambda_+} - \sqrt{\epsilon^2 - \lambda_-}) l / (2 \hbar c) \right), \quad (3.2)$$

where m_ϕ is the mass of the axion, ϵ is the energy of the photon, $\mu = |\mathbf{B}| / (M_L c^2)$ and $\lambda_\pm = (m_\phi^2 \pm \sqrt{m_\phi^4 + 4 \mu^2 \epsilon^2 / c^8}) / 2$ are the squared-mass eigenvalues [5]. Note that despite the fact that $\lambda_- < 0$, that mode has positive energy when the energy ϵ is taken into account.

If $\mu \ll m_\phi c^2$ then there are two distinct energy regimes:

- High energy photons ($\epsilon \gg m_\phi^2 c^4 / \mu$), for which the oscillation is maximal and achromatic:

$$P_{\gamma \rightarrow \gamma}(l) = 1 - \sin^2 (\mu l / (2 \hbar c)) \quad (3.3)$$

- Low energy photons ($m_\phi c^2 \ll \epsilon \ll m_\phi^2 c^4 / \mu$), for which the oscillation is small and energy-dependent:

$$P_{\gamma \rightarrow \gamma}(l) = 1 - 4 \frac{\mu^2 \epsilon^2}{m_\phi^4 c^8} \sin^2 (m_\phi^2 c^3 l / (4 \hbar \epsilon)) \quad (3.4)$$

In the Universe, the intergalactic magnetic field is not uniform but is assumed by CKT to vary in domains of size $L_{\text{dom}} \sim 1 \text{Mpc}$, which is much smaller than the distance

⁽²⁾ Throughout the paper, we will use some electromagnetic units such that both the electric and magnetic fields have the dimension of an energy square while the axion scalar field has the dimension of an energy. This means that the magnetic field in SI units is given by $B_{SI} = |\mathbf{B}| / \text{Sqrt}4\pi\epsilon_0\hbar^3c^5/\alpha$. The speed of light will be denoted by c , the Newton's constant by \mathcal{G}_N , the vacuum permittivity by ϵ_0 and the fine-structure constant by $\alpha = 1/137$.

to high redshift SNe ($z \sim 1$ is equivalent to distances about 10^4 Mpc). CKT assume a uniform distribution of randomly oriented magnetic fields over the 1 Mpc domains⁽³⁾. In that case high energy unpolarized photons (as defined above) approach an equilibrium population evenly divided between the two photon polarizations and the axion at large distances. CKT found that the approach to equilibrium is through an exponential damping of the number of high energy photons [5]:

$$P_{\gamma \rightarrow \gamma}(l) \simeq \frac{2}{3} + \frac{1}{3} e^{-l/L_{\text{dec}}}, \quad (3.5)$$

where the decay length is approximatively given by:

$$L_{\text{dec}} = \frac{8}{3} \frac{\hbar^2 c^6 M_L^2}{L_{\text{dom}} |\mathbf{B}|^2}. \quad (3.6)$$

Before studying the implications of this photon loss mechanism on the SN data, it is worth mentioning how to evade any unwanted effects on the CMB anisotropy. While the photons of the CMB were emitted at energies of the atomic sizes, when the magnetic field appears they have already redshifted down to much lower energies about 10^{-4} eV. In this low energy regime, the oscillation mixing is energy suppressed and requiring $1 - P_{\gamma \rightarrow \gamma}$ to be less than the CMB anisotropy (10^{-5}) gives a lower bound on the axion mass around $m_\phi > 10^{-16}$ eV [5].

4 Cosmography: luminosity distance vs. redshift with and without photon loss

Let us now study the consequences of this photon loss mechanism on the measures of the luminosity distances. A nice review for non-specialists of the cosmological parameters and their determination can be found in [23].

A homogeneous and isotropic space, as our Universe appears to be at large scales, is described by the Robertson–Walker metric

$$ds^2 = -c^2 dt^2 + R_\circ^2 a^2(t) \left(\frac{dr^2}{1 - kr^2} + r^2 d\theta^2 + r^2 \sin^2 \theta d\phi^2 \right) \quad (4.7)$$

where $a(t)$ is the dimensionless scale factor (by convention $a(\text{today}) = 1$), R_\circ characterizes the absolute size of the Universe, while with an appropriate rescaling of the coordinates the curvature parameter k takes values $+1, 0, -1$ for closed, flat and open universes.

For energy-momentum sources made of a superposition of perfect fluids specified by their energy densities ρ_i and their pressures p_i , the Einstein equations reduce to the

⁽³⁾As mentioned earlier, these magnetic fields are poorly understood and may be distributed much more irregularly than is assumed here. We thank Hui Li for a discussion of this point.

Friedmann equation (a dot stands for a derivative with respect to the time coordinate):

$$H^2 = \frac{8\pi\mathcal{G}_N}{3} \sum_i \rho_i - \frac{kc^2}{a^2 R_o^2}, \quad \text{where } H = \frac{\dot{a}}{a} \quad (4.8)$$

together with the conservation equation:

$$\dot{\rho}_i + 3(\rho_i + p_i)H = 0 \quad (4.9)$$

It is common to introduce the ratio of the energy densities to the critical energy density for a flat universe:

$$\Omega_i = \frac{8\pi\mathcal{G}_N \rho_i}{3H^2} \quad \text{and} \quad \Omega_{\text{curv.}} = -\frac{kc^2}{a^2 R_o^2 H^2} \quad (4.10)$$

Note that $\sum_i \Omega_i + \Omega_{\text{curv.}} = 1$ by (4.8). In terms of the redshift parameter $z = 1/a - 1$ (by convention, since $a_0 = 1$, $z_0 = 0$) and assuming a constant equation of state $p_i = w_i \rho_i$ for each component of the stress-energy tensor, the conservation equation (4.9) can be integrated with respect to time, giving a relation between the densities ρ_i , the scale factor a and the equation of state w_i . This gives,

$$\rho_i = \rho_{0i} (1+z)^{3(1+w_i)}. \quad (4.11)$$

The Friedmann equation (4.8) can then be rewritten ⁽⁴⁾:

$$H^2(z) = H_0^2 (1+z)^2 \left(1 + \sum_i \Omega_i ((1+z)^{1+3w_i} - 1) \right) \quad \text{and} \quad 1 - \sum_i \Omega_i = -\frac{kc^2}{R_o^2 H_0^2} \quad (4.12)$$

A crucial test of cosmological models comes from Hubble diagrams for standard candles by plotting their luminosity distances versus their redshifts. The luminosity distance is defined by considering a source located at the comoving distance r_s , which has emitted some light at a time t_s with an absolute luminosity \mathcal{L} (energy per time produced by the source, normalized to that of a standard candle). This light is detected today by a detector located at $r = 0$ which measures a flux \mathcal{F} (energy per time per area) and a redshift z_s . Taking into account the energy loss due to the redshift of the light and the increase of time intervals between the emission and the reception, the conservation of energy ensures that,

$$\mathcal{L} = 4\pi r_s^2 R_o^2 (1+z_s)^2 \mathcal{F}. \quad (4.13)$$

The luminosity distance between the source and the detector is defined by,

$$\mathcal{L} = 4\pi d_L^2 \mathcal{F}. \quad (4.14)$$

⁽⁴⁾From now we will omit the subscript 0 on the energy density ratios Ω_i evaluating those quantities only at the present time.

The quantities characterizing the source are not independent but can be related to each other through the ratios Ω_i governing the dynamical evolution of the Universe. This is why the independent measurement of two supernova observables can tell us about Sandage's numbers. The trajectory of light is given by the null geodesic equation, $ds^2 = 0$, which when integrated becomes,

$$\int_0^{r_s} \frac{dr}{\sqrt{1 - kr^2}} = \int_{t_s}^{\text{today}} \frac{c dt}{R_\circ a(t)} = \int_0^{z_s} \frac{c dz}{R_\circ H(z)} \quad (4.15)$$

Using (4.12) this integral equation can be solved to relate the comoving distance r_s of the source to its redshift⁽⁵⁾:

$$r_s(z_s) = \text{sinn} \left(\frac{c}{R_\circ H_0} \int_0^{z_s} \frac{dz}{(1+z) \sqrt{1 + \sum_i \Omega_i ((1+z)^{1+3w_i} - 1)}} \right) \quad (4.16)$$

This relation allows one to predict the luminosity distance of the source in terms of its redshift:

$$d_L = (1 + z_s) r_s(z_s) R_\circ. \quad (4.17)$$

So far this expression has been derived assuming that once emitted the light propagates freely in all spatial directions. The CKT proposal that photons can disappear into axions in the intergalactic magnetic field changes the relation (4.17) for $d_L(z_s)$. Imagine indeed that over the distance $r_s R_\circ$ a fraction $(1 - P_{\gamma \rightarrow \gamma}(r_s R_\circ))$ of the number of photons has decayed into axions, thus only a fraction $P_{\gamma \rightarrow \gamma}(r_s R_\circ)$ of the energy emitted by the source will be detected and the conservation equation (4.13) has to be modified accordingly:

$$\mathcal{L} = 4\pi r_s^2 R_\circ^2 (1 + z_s)^2 \mathcal{F} / P_{\gamma \rightarrow \gamma}(r_s R_\circ) \quad (4.18)$$

Then the expression for the luminosity distance as a function of the redshift becomes:

$$d_L = \frac{(1 + z_s) r_s(z_s) R_\circ}{P_{\gamma \rightarrow \gamma}^{1/2}(r_s(z_s) R_\circ)} \quad (4.19)$$

where $r_s(z_s)$ is still given by (4.16). Usually, the data are not presented in terms of $d_L(z_s)$ but rather in terms of the magnitude defined as

$$m = m_0 + 5 \log_{10}(H_0 d_L / c) \quad (4.20)$$

where m_0 is the magnitude associated to the absolute luminosity of the source (after corrections deduced from the fitting to the Phillips curve, m_0 is the common quantity to all SNe and it is fit to the data).

⁽⁵⁾The definition of the function ‘sinn’ depends on the topology of the Universe: $\text{sinn}x = \sinh x$, $x, \sin x$ for an open, flat, closed Universe, see for instance citeCPT.

We would like to comment briefly on the effect of photon loss on the measured flux. The luminosities of distant supernovae fluctuate too much in general for such supernovae to make good standard candles. However, it has been noticed that the absolute luminosities of Type Ia supernovae can be determined by fitting the time evolution of the measured SN luminosity to the phenomenological Phillips curve [11]. Roughly speaking, the broader the light curves of a Type Ia supernova, the brighter it is intrinsically. Given the absolute luminosity, together with the measured luminosity, one determines a normalized flux \mathcal{F} . The effect of photon loss is to reduce the measured flux, but it is important that the Phillips curve not change as a result. The first point is that the Phillips curve measures brightness on a logarithmic scale as a function of the age of the supernova. Hence, if a fraction of photons is lost by a particular source, the light curve will simply be shifted vertically. This is the effect we have been discussing. The only reason for concern is then whether or not the broadness of the observed light curve should change as a result of photon loss, as that is how the absolute luminosity of a Type Ia supernova is determined. The luminosity signal is generally high enough above background that we believe this will be a negligible effect. A more precise analysis remains to be done, however.

The CKT model described above provides a physical example of a photon loss mechanism in which the $P_{\gamma \rightarrow \gamma}$ probability is directly related to particle physics parameters that can therefore be constrained by the SN data.

What the supernova data indicate (Figure 1) is that supernovae with $z \sim 1$ are dimmer than can be explained by a universe with only ordinary matter in it ($w_M = 0$), assuming no loss of photons. The universe undergoes a period of acceleration if the Dark Energy has an equation of state $w_X < -1/3$ (the condition for having an accelerating period of acceleration today is $\omega_X < -1/(3 - 3\Omega_m)$ and if $-1/(3 - 3\Omega_m) < \omega_X < -1/3$ will accelerate in the future). Suppose we choose to assume that there is no period of acceleration. Then we can study the requirements of a photon loss mechanism to explain the supernova data. We think it is worth studying such generalizations because the authors of [5] make many assumptions regarding observational astrophysics which are not well understood. For example, as mentioned earlier, the structure of the intergalactic magnetic field may be significantly different than the CKT assumption of 1 Mpc domains of constant magnitude. Furthermore, there may be other acceptable photon loss mechanisms, either via new particle physics or via uniform absorption by an unknown intergalactic medium.

For $z < 1$ we require that the photon loss be so as to force a positive slope for the magnitude-redshift curve. For example, in the absence of a photon loss mechanism, the dotted curve in Figure 1 must be forced upward. The supernova magnitude is proportional to the logarithm of its luminosity, so by (4.18) this magnitude is shifted by the addition of a term proportional to $\log(P_{\gamma \rightarrow \gamma})$. If we assume that for low z , $P_{\gamma \rightarrow \gamma} \sim 1 - \delta P_{\gamma \rightarrow \gamma}(z)$ where $\delta P_{\gamma \rightarrow \gamma}(z) \ll 1$, then we require that $\delta P_{\gamma \rightarrow \gamma}(z)$ have a linear term which can control the slope of the magnitude-redshift curve. Otherwise a fit will likely become more difficult. The other requirement is that if we want to match onto the single Type Ia observation at $z \sim 1.7$ [24], then the magnitude-redshift curve must

be allowed to slope downward by then. The easiest way to accomplish this is to give $\log(P_{\gamma \rightarrow \gamma}(z))$ a small negative slope and positive second derivative near $z \sim 1$. These requirements are satisfied by the CKT mechanism. We have also checked that in a variety of phenomenological photon loss models (without theoretical basis) for which these two requirements are satisfied, it is rather easy to fit the supernova data at least as well as the accelerating universe by a cosmological constant.

5 Statistical fits

In this section we describe the statistics behind our χ^2 fits for the parameters in the generalized CKT model. We have included a total of 18 supernovae from the Calán-Tololo Supernova Survey [6] and 36 from the Supernova Cosmology Project [2]. Following [2] we removed six outlying data points of their 42 total, corresponding to their Fit C. Furthermore, in the fits presented here we have tentatively dropped the $z \sim 1.7$ point [24] because of its large error bars compared to the remaining data. We have checked that the results are nearly unchanged when that point is included.

In our fits we have assumed a two component flat universe with a fractional density Ω_m of ordinary matter and $\Omega_X = 1 - \Omega_m$ of Dark Energy with equation of state $p_X = w_X \rho_X$. We assume the CKT model for photon loss parametrized by the photon decay length L_{dec} . For the SCP data we use their correlated error matrix as presented at <http://www-supernova.lbl.gov>.

The data are displayed together in Figure 1, together with magnitude-redshift curves of various models including the CKT model. The data are displayed in terms of residual magnitudes with respect to the SCP flat accelerated universe with $\Omega_m = .28$, $\Omega_X = .72$, $w_X = -1$. The CKT model differs only slightly from the SCP model for small z . Notice that at very large z there is a deviation in magnitude of around .1 between the CKT model and the SCP accelerated universe. In the limit of large z this deviation depends on the photon decay length and is larger for a smaller decay length. Note also that for $1 < z < 5$ the CKT magnitude dips below the SCP accelerated universe. These facts may allow the models to be distinguished if better high- z data is obtained.

Figure 2 demonstrates the maximum likelihood regions for a flat universe with the CMB preferred value $\Omega_m = 0.3$ in terms of L_{dec} and w_X . Note that at the one sigma level the accelerating universe and the CKT point are equally good fits to the data. Also note that even with the photon loss, negative values for w_X are strongly favored which is an independent result consistent with the constraints coming from the CMB anisotropies. However, the allowed region for w_X consistent with CMB constraints is quite large over reasonable values of the photon decay length.

In Figure 3 we give the confidence plots for a flat universe with matter component Ω_m and Dark Energy equation of state parameter w_X . In the lower two panels a best fit is taken over photon decay parameter L_{dec} . Typical values for L_{dec} can be read off of Figure 2. We note that the likely region for w_X opens dramatically, even if we confine ourselves to the CMB preferred matter density $\Omega_m = 0.3$.

Figure 4 demonstrates the enlarged region of allowed values in the $\Omega_m - \Omega_\Lambda$ plane assuming a cosmological constant for the Dark Energy ($\omega_\Lambda = -1$). In this case the dimming of supernovae is a combined effect of acceleration and the CKT photon loss mechanism.

6 Conclusions

We have presented an analysis of the SN data taking into account a photon loss mechanism as recently proposed by CKT. This mechanism offers a new parameter, namely the photon decay length, to accomodate the data. The main conclusion of our analysis, as already announced by CKT, is that the dimming of SNe at large redshift no longer requires an accelerating expansion of the Universe, and the photon-axion coupling opens up the window for the equation of state of the Dark Energy towards less negative values. We argue that the accelerating universe and the CKT models may be distinguishable if better high- z data becomes available. In this way future experiments like MAP and SNAP may reveal new physics beyond the standard models of both particle physics and cosmology. In the new allowed region of the parameter space, the SN data could not only confirm the existence of a Dark Energy component but may also reveal the existence of a light pseudoscalar that has so far evaded any direct particle physics detection.

Acknowledgments

We are especially grateful to Csaba Csáki, Nemanja Kaloper and John Terning for sharing their work prior to publication, and for many interesting discussions. We are also happy to thank Tanmoy Bhattacharya, Guillaume Blanc, Salman Habib and Hui Li for useful discussions. C.G. thanks the hospitality of the T-8 group at Los Alamos, where this work was performed. J.E. is supported in part by the US Department of Energy under contract W-7405-ENG-36.

References

- [1] A. G. Riess *et al.* [Supernova Search Team Collaboration], *Astron. J.* **116**, 1009 (1998) [[astro-ph/9805201](#)].
- [2] S. Perlmutter *et al.* [Supernova Cosmology Project Collaboration], *Astrophys. J.* **517**, 565 (1999) [[astro-ph/9812133](#)].
- [3] S. Weinberg, *Rev. Mod. Phys.* **61**, 1 (1989); E. Witten, [hep-ph/0002297](#); S. M. Carroll, *Living Rev. Rel.* **4**, 1 (2001) [[astro-ph/0004075](#)]; S. Weinberg, [astro-ph/0005265](#).

- [4] T. Banks, [hep-th/0007146](#); T. Banks and W. Fischler, [hep-th/0102077](#); S. Hellerman, N. Kaloper and L. Susskind, *JHEP* **0106**, 003 (2001) [[hep-th/0104180](#)]; W. Fischler, A. Kashani-Poor, R. McNees and S. Paban, *JHEP* **0107**, 003 (2001) [hep-th/0104181](#); T. Banks and M. Dine, *JHEP* **0110**, 012 (2001) [[hep-th/0106276](#)].
- [5] C. Csáki, N. Kaloper and J. Terning, [hep-ph/0111311](#).
- [6] M. Hamuy *et al.* [Caán–Tololo Survey], *Astrophys. J.* **106**, 2392 (1993).
- [7] A. Aguirre and Z. Haiman, [astro-ph/9907039](#) J. T. Simonsen and S. Hannestad, *Astron. Astrophys.* **351**, 1 (1999) [[astro-ph/9909225](#)]; T. Totani and C. Kobayashi, *Astrophys. J.* **526**, L65 (1999) [astro-ph/9910038](#).
- [8] M. S. Turner and M. J. White, *Phys. Rev. D* **56**, 4439 (1997) [[astro-ph/9701138](#)]; D. Huterer and M. S. Turner, [astro-ph/0012510](#).
- [9] S. Perlmutter, M. S. Turner and M. J. White, *Phys. Rev. Lett.* **83**, 670 (1999) [[astro-ph/9901052](#)].
- [10] C. B. Netterfield *et al.* [Boomerang Collaboration], [arXiv:astro-ph/0104460](#); *see also* P. de Bernardis *et al.* [Boomerang Collaboration], *Nature* **404**, 955 (2000) [astro-ph/0004404](#); S. Hanany *et al.*, *Astrophys. J.* **545**, L5 (2000) [astro-ph/0005123](#); C. Pryke, N. W. Halverson, E. M. Leitch, J. Kovac, J. E. Carlstrom, W. L. Holzapfel and M. Dragovan, [astro-ph/0104490](#).
- [11] M. M. Phillips *Astrophys. J. Lett.* **413**, L105 (1993).
- [12] S. T. Myers, J. E. Baker, A. C. Readhead, E. M. Leitch and T. Herbig, *Astrophys. J.* **485**, 1 (1997) [[astro-ph/9703123](#)].
- [13] S. Moriyama, M. Minowa, T. Namba, Y. Inoue, Y. Takasu and A. Yamamoto, *Phys. Lett. B* **434**, 147 (1998) [[hep-ex/9805026](#)].
- [14] G. G. Raffelt, *Chicago, USA: Univ. Pr. (1996) 664 p.*
- [15] M. S. Turner, *Phys. Rept.* **197**, 67 (1990); G. G. Raffelt, *Phys. Rept.* **198**, 1 (1990).
- [16] M. T. Ressell, *Phys. Rev. D* **44**, 3001 (1991).
- [17] S. R. Furlanetto and A. Loeb, [astro-ph/0102076](#).
- [18] Yu. N. Gnedin, [astro-ph/0111316](#).
- [19] P. P. Kronberg, *Space Sci. Rev.* **75**, 387 (1996).
- [20] A. D. Dolgov and D. Grasso, [astro-ph/0106154](#).

- [21] D. Grasso and H. R. Rubinstein, Phys. Rept. **348**, 163 (2001) [[astro-ph/0009061](#)].
- [22] P. Sikivie, Phys. Rev. Lett. **48**, 1156 (1982); H. Georgi, P. Ginsparg and S. L. Glashow, Nature **306**, 765 (1983).
- [23] P. B. Pal, Pramana **54**, 79 (2000) [[hep-ph/9906447](#)].
- [24] A. G. Riess *et al.*, [astro-ph/0104455](#).
- [25] S. M. Carroll, W. H. Press and E. L. Turner, Ann. Rev. Astron. Astrophys. **30**, 499 (1992).

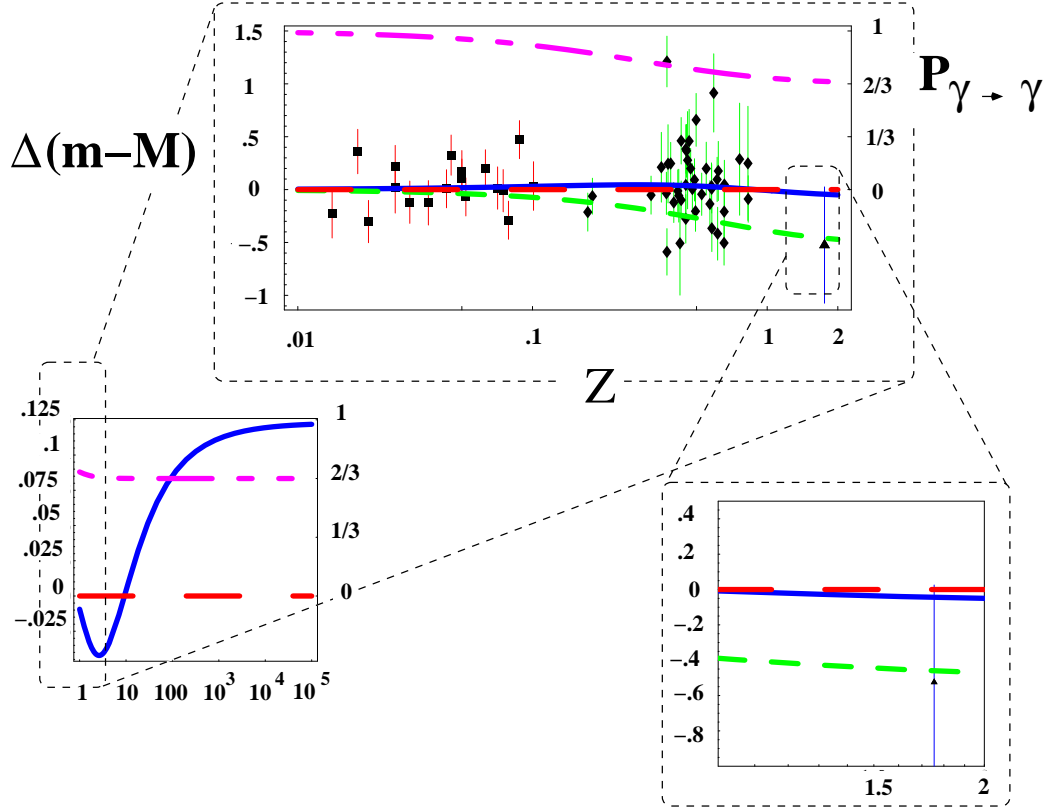


Figure 1: Hubble diagram for the type Ia supernovae. The residual magnitudes from the best-fit flat cosmology with a cosmological constant and no photon loss (the “SCP accelerated universe”) are plotted. The box points are the 18 supernovae from the Calán–Tololo Supernova Survey [6], the diamond points are the 42 supernovae from the Supernova Cosmology Project [2] and the triangle point is the farthest known Type Ia supernova observed by the Hubble Space Telescope [24]. The dashed line is the theoretical curve for the best-fit flat accelerated cosmology with no axion-photon mixing $(\Omega_m, \Omega_X, w_X) = (.28, .72, -1)$; the solid line is the theoretical curve for the flat cosmology with a choice of photon-axion mixing parameter $(\Omega_m, \Omega_X, w_X, L_{\text{dec}} H_0/c) = (.3, .7, -1/3, 1/3)$; the lower dashed line shows the effect of turning off the photon-axion coupling with the otherwise identical choice of parameters. Finally, the upper dot-dot-dashed line is the remaining photon intensity probability on a distance $r_s(z)R_\odot$, with the probability scale given to the right of the plot. The lower left plot emphasizes the very high z behavior; the upper plot focuses on the region where the SNe are observed; and the lower right plot enlarges the region near the farthest supernova.

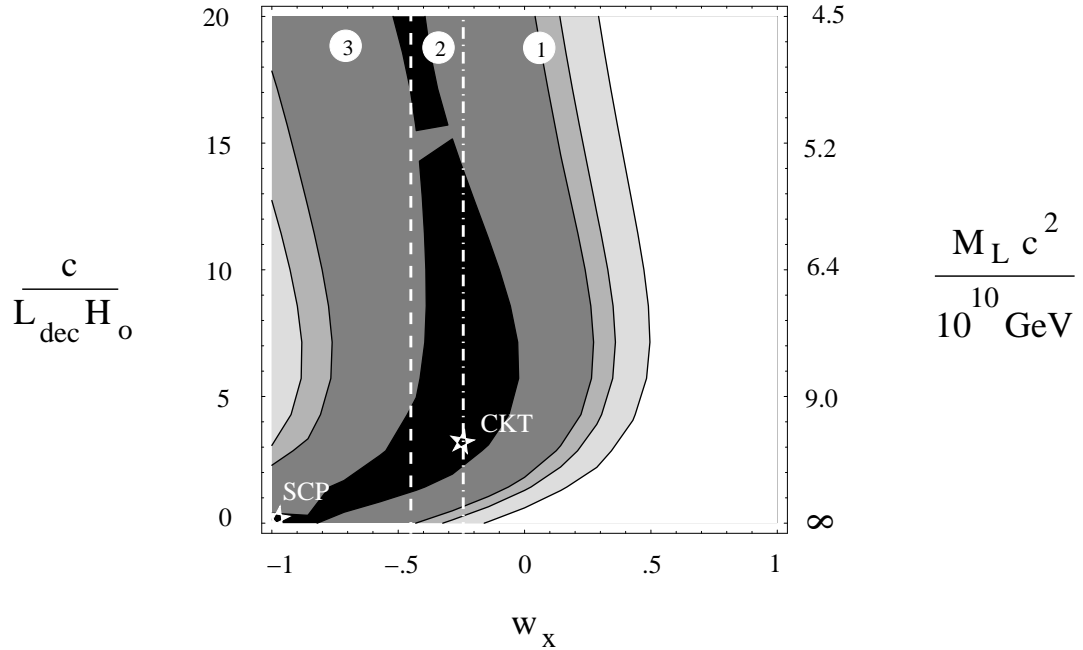


Figure 2: From black to white: 68%, 90%, 95% and 99% confidence regions in the $(w_X - c/L_{dec}H_0)$ plane for a flat Universe formed of matter with $\Omega_m = .3$ and an additional Dark Energy component with an equation of state w_X . The χ^2 on the right correspond to a data set of 54 points as described in the text. For a given amplitude of the intergalactic magnetic field and a given length of coherence for it, the decay length is proportional to the square of the axion coupling scale M_L (the values reported on the right correspond to $B = 10^{-13}$ Tesla and $L_{dom} = 1$ Mpc). The two stars in the plot are the SCP accelerated universe with a cosmological constant ($w_X = -1$, $L_{dec} = \infty$) and the CKT universe with cosmic strings and a photon-axion coupling ($w_X = -1/3$, $L_{dec}H_0/c \sim 3$). The dashed and dot-dashed lines separate regions of present acceleration (3), present deceleration but future acceleration (2) and eternal deceleration (1). We note that the accomodation of the SN data by a photon loss mechanism does not require the universe to accelerate.

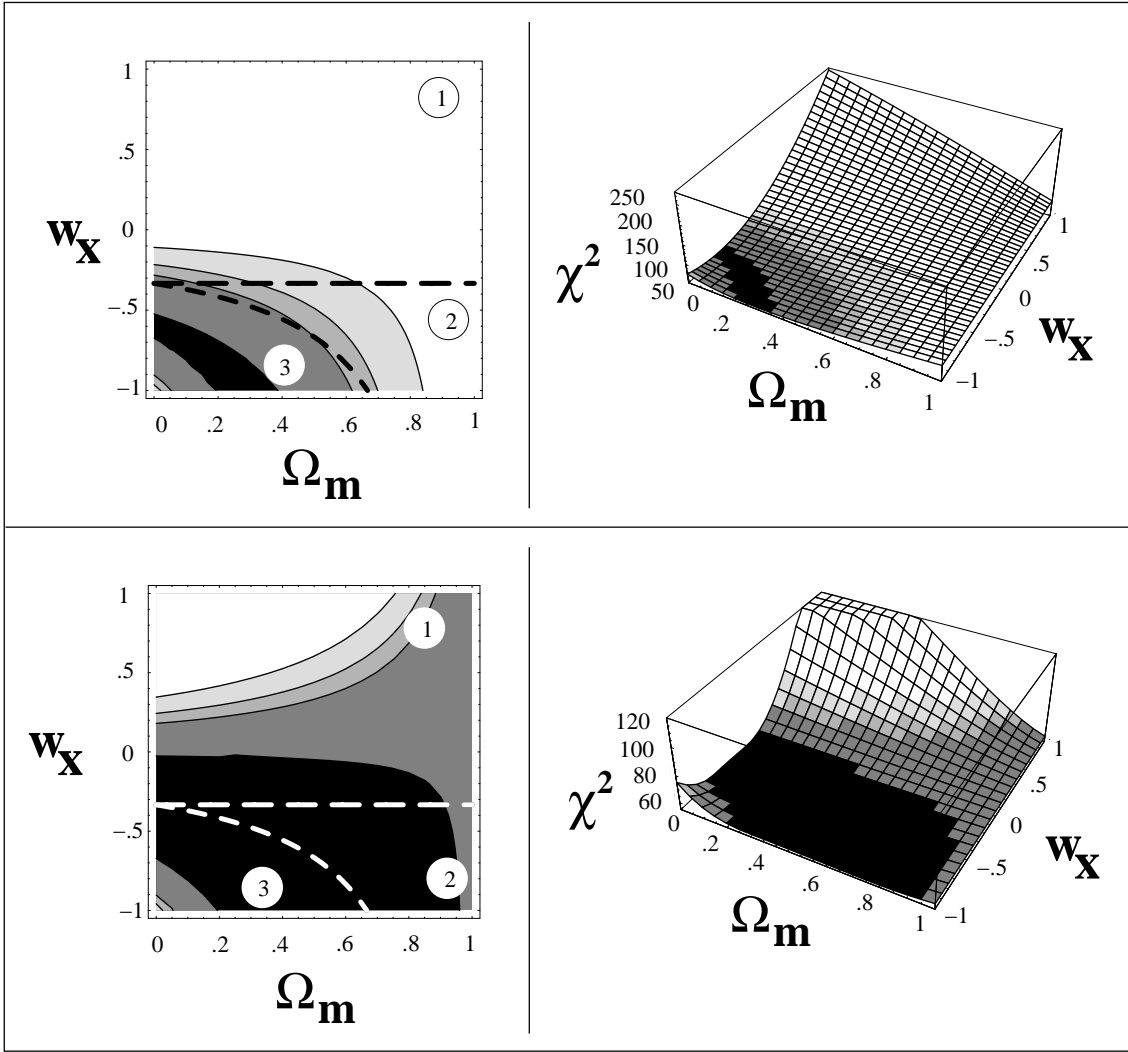


Figure 3: Best-fit, from black to white: 68%, 90%, 95% and 99% confidence regions in the $(\Omega_m - w_X)$ plane for a flat Universe, *i.e.* $\Omega_X = 1 - \Omega_m$, formed of matter and an additional Dark Energy component with an equation of state w_X . The upper plots are obtained in the standard model without mixing between photons and axions, the lower ones show the modifications due the photon loss mechanism. The dashed and dot-dashed lines separate regions of present acceleration (3), present deceleration but future acceleration (2) and eternal deceleration (1). While within the usual interpretation of the SN data a period of present acceleration is prefered at 90%, the second plots show that if a photon-axion mixing is accounting for the dimming of the data a large z it can perfectly accommodate a cosmological evolution without any period of present or future acceleration.

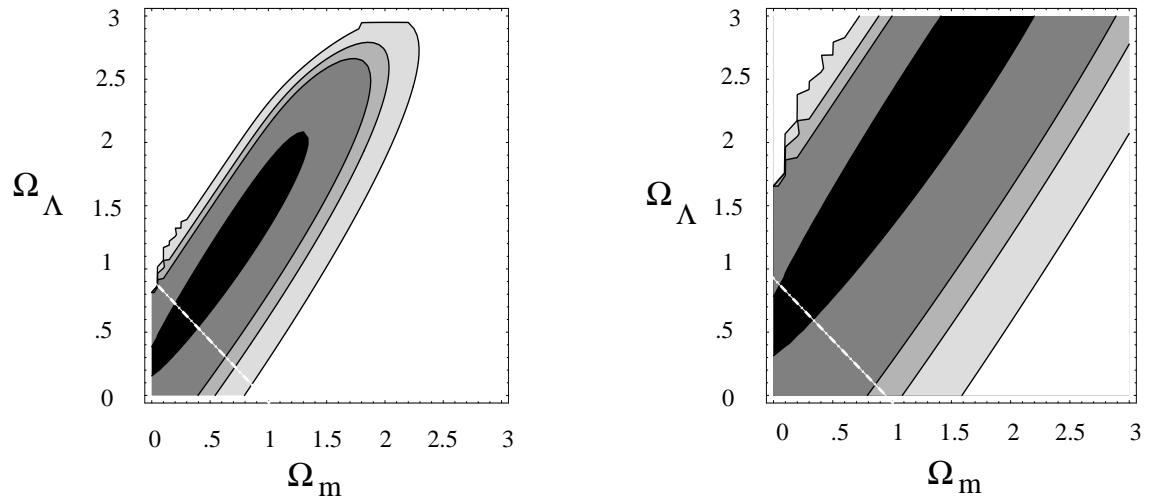


Figure 4: Best-fit, from black to white: 68%, 90%, 95% and 99% confidence regions in the $(\Omega_m - \Omega_\Lambda)$ plane for a Universe formed of matter and an additional cosmological constant component with an equation of state $w = -1$. The comparison of the two plots shows the influence of the photon loss mechanism (on the left the decay length of the photon is set to infinity while on the right it is fit to its best χ^2 value at each point). The dot-dashed lines locate flat universes.